Effects of stochastic forces on the nonlinear behaviour of a silicon nitride membrane nanoelectromechanical resonator

Sri Saran Venkatachalam, Xin Zhou

Effects of stochastic forces on the nonlinear behaviour of a silicon nitride membrane nanoelectromechanical resonator

Srisaran Venkatachalam and Xin Zhou*
CNRS, Université Lille, Centrale Lille,Université Polytechnique Hauts-de-France, UMR8520, IEMN, Av. Henri Poincare, Villeneuve d'Ascq 59650, France
(Dated: February 28, 2023)

In this work, we present the effects of stochastic force generated by white noise on the nonlinear dynamics of a circular silicon nitride membrane. By tuning the membrane to the Duffing nonlinear region, detected signals switching between low- and high-amplitudes have been observed. They are generated by noise-assisted random jumps between bistable states at room temperature and exhibit high sensitivity to the driving frequency. Through artificially heating different mechanical vibration modes by external input of white noise, the switching rate exhibits exponential dependence on the effective temperature and follows with Kramer's law. Furthermore, both the measured switching rate and activation energy exhibit sensitivity to the width of the hysteresis window in nonlinear response and the driving force, which is in qualitative agreement with the theoretical descriptions. Besides, white noise-induced hysteresis window squeezing and bifurcation point shifting have also been observed, which are attributed to the stochastic force modulation of the spring constant of the membrane. These studies are carried out in an all-electric operating scheme at room temperature, paving the way for the exploration of probability distribution-based functional elements that can be massively integrated on-chip.

Keywords: stochastic switching, Duffing nonlinearity, silicon nitride membrane, nanoelectromechanical resonator

I. INTRODUCTION

Stochastic switching between coexisting states has been observed in chemistry, physics, biology, and engineering systems. Its mechanism can be explained simply through descriptions of a fictive particle hopping randomly in bistable states of a double-well potential [1]. Although these individual switching events are random, both distribution and probability of switching can be well predicted and controlled, exhibiting several potential applications. For instance, it brings an enhancement of signal-to-noise ratio [2] and random number generators [3], which could offer a means of enhancing signal processing . Besides, stochastic switching can directly perform stochastic computing, which are attractive for novel error-tolerant computing schemes in neuromorphic applications [4, 5]. Therefore, reserach interests are preserved in exploring stochastic switching in various systems, including Josephson junctions [6, 7], protein folding [8], nanomagnets [9, 10].

Micro- or nano-mechanical resonator, which allows electrical and optical signals to couple with a mechanical degree of freedom, is one of interesting components for exploring stochastic switching [11, 12]. Because of intrinsic nonlinearity coming from geomentry, nano-mechanical resonators can be driven as Duffing oscillators, providing the indispensable condition: bistable states. In addition, the idea of building multifunctional components based on nanoelectromechanical resonators has been driving researchers to explore fundamental aspects and potential applications beyond sensing [13–17]. So far, white noise assisted stochastic switching has been investigated by using cantilevers [12], double-clamped beams [18, 19], and membranes [20, 21]. In these previous studies, nanomechanical resonators were operated using either magnetomotive detection at low temperature or optical readout at room temperature, which are not conducive to the further development of functional elements based on stochastic switching that can be integrated in large quantities on-chip. In very recent years, high-stress silicon nitride membrane electromechanical resonators emerge and offer high quality factors with resonance frequency in MHz ranges. They allow vibrating membranes to be strongly coupled to external electronic circuits, providing a highly sensitive actuation and detection scheme at room temperature [22–24]. However, to date there are few studies of the effect of stochastic forces generated by white noise on the nonlinear behaviour of such membrane nanoelectromechanical resonators in a fully electric operating scheme at room temperature.

In this work, we present experimental studies of stochastic switching in a circular membrane nanoelectromechanical resonator, which consists of a silicon nitride drum, capacitively coupled to a suspended aluminum gate. At the room temperature experiment, the membrane resonator is frequency biased in Duffing nonlinear region, creating bi-stable states for mechanical displacements. The membrane is artificially heated by adding external white noise, and the switching rate of different mechanical modes as a function of the effective temperature has been measured. Its characteristics follow Kramer's law. Experimental parameters affect on this noise assisted jumping between bistable states have been analyzed by comparing our measurements with the theoretical descriptions. Besides, squeeze of hysteresis

* Corresponding Author: xin.zhou@cnrs.fr

window in nonlinear responses has also been observed when the amplitudes of stochastic force increases.

II. METHODS

The device measured in this experiment is a silicon nitride membrane electromechanical resonator. It consists of a silicon nitride circular membrane with ~ 33 μm in diameter and ~ 80 nm in thickness, which is fabricated based on a substrate composed of a high tensile stress (~ 1 GPa) silicon nitride thin film on top of the silicon wafer. The membrane is covered with an aluminum thin film, ~ 25 nm in thickness, and is capacitively coupled to a suspended aluminium top-gate, as shown in Fig.1 (a). The distance between the membrane and its gate is $d \approx 600$ nm. Details of the fabrication process have been reported in the previous work [22, 23]. In this room temperature measurement, the membrane is set in a vacuum chamber ($\sim 10^{-6}$ mbar) and grounded through its top gate. In this capacitive coupling scheme, mechanical displacement x can be excited by an electrostatic force $f_d(t)$, which is generated through combining a dc signal V_{dc} and a ac signal with a frequency Ω, $V_{ac} \cdot cos(\Omega \cdot t)$, which gives $f_d = \frac{1}{2}\partial(C_g(x)(V_{dc}+V_{ac}\cdot cos(\Omega\cdot t))^2)/\partial x$. The $C_g(x)$ is the coupling capacitance between the membrane and its gate, and the $x(t)$ is the mechanical displacement. To study noise assisted random jumps between bistable states, white noise that is generated by an arbitrary waveform generator is injected to the membrane resonator, through a band-pass filter centred at the desirable frequency corresponding to the resonant mechanical mode. It yields the stochastic force $f_n(t)$ also driving on the membrane. Therefore, the mechanical displacement $x(t)$ of this circular membrane can be described by a motion equation Eq.1,

$$m_{eff}(\ddot{x} + \gamma_m \dot{x} + \Omega_m^2 x + \frac{\alpha}{m_{eff}} x^3) = f_n(t) + f_d(t). \quad (1)$$

Here, Ω_m is the resonance frequency of mechanical resonator, the γ_m is the linewidth, α is the Duffing coefficient, and m_{eff} is effective mass of the membrane. The α/m_{eff} term is the Duffing coefficient normalized with the effective mass, having the unit $m^{-2}s^{-2}$. For circular membrane resonators, the mechanical mode is designated by (i, j), where azimuthal mode number is indexed by the i (= 0, 1, ...) and the radial mode number is denoted by the j (= 1, 2, ...). In the following discussions, these parameters corresponding to the mechanical vibration modes will be specified.

A detection scheme is built on microwave interferometry, in which the tiny mechanical displacements excited by $f_d[\Omega]$ are transduced by a microwave signal with frequency ω to be the signal having frequency at $\omega + \Omega$. The displacement $x(t)$ is readout by a lock-in amplifier through a frequency down-conversion. The details of both driving and detection schemes are shown in 1 (b). The microwave interferometry allows to transduce the detected amplitude of electrical signals into mechanical displacement x by using the relation $V_{out} = G\omega Z_0 C_g x V_{\mu w}/(2d)$ [22]. Here, the $Z_0 = 50$ Ohm is the impedance of the measurement line, $C_g \approx 10$ fF is the capacitance between the membrane and its coupled gate, $V_{\mu w}$ is the input amplitude of microwave signal for detection (in this measurement, $V_{\mu w} \approx 300$ mV_p), the V_{out} is the detected amplitude of the microwave signal, and the G is the total gain in the detection chain in this experiment.

Figure 1 (c) shows linear responses of the mechanical fundamental mode (black line), whose resonance frequency is $\Omega_m/2\pi \approx 11.781$ MHz with linewidth $\gamma_m/2\pi = 1015$ Hz. When the mechanical resonator is driven by a periodic force with a large amplitude, the spring hardening ($\alpha > 0$) makes the resonance frequency shift towards the higher values and frequency responses exhibit hysteric behavior between forward (red line) and backward (blue line) frequency sweeps. Bistable states exist in this region, which is defined between two saddle-node bifurcation points corresponding to the amplitude of mechanical response jump-down Ω_{bd} in the forward frequency sweep and jump-up Ω_{bu} in the backward sweep [12, 18, 19]. It is a typical Duffing nonlinear phenomenon and has been observed in various mechanical resonators. Besides, the spectral density of the electromechanical resonator's amplitudes, driven by white noise in the form of stochastic force f_n with different power, has also been measured, as shown in Fig.1 (d). The spectral of stochastic force is given by $S_{ff}(\Omega) = \int < f_n(t) f_n(0) > e^{i\Omega t} dt$, exciting mechanical displacement and creating spectrum $S_{xx}(\Omega) = |\chi_m(\Omega)|^2 S_{ff}(\Omega)$. The $\chi_m(\Omega)$ is the susceptibility of the membrane resonator, $\chi_m(\Omega) = \frac{1}{2m_{eff}\Omega_m(\Omega_m - \Omega - i\gamma_m/2)}$. It is well-known that the integration of the S_{xx} allows to access the mean square amplitude $< x(t)^2 >$, $< x(t)^2 > = \frac{1}{2\pi}\int S_{xx}(\Omega) d\Omega$. According to equipartition theorem [25–28], the effective temperature T_e of the mechanical resonator driven by stochastic forces, in the classical limit, is described by Eq.2,

$$T_e = \frac{m_{eff}\Omega_m^2 < x(t)^2 >}{k_B}. \quad (2)$$

The k_B is the Boltzmann constant. In our measurement, the measured spectral (shown in Fig.1 (d)) can be converted into displacement spectral density S_{xx} according to the basic principle of microwave interferometry mentioned above [22]. Then, by integration of the measured S_{xx}, the T_e is obtained based on the Eq.2. The corresponding effective temperatures are marked in Fig. 1 (d), which are obtained based on these expressions by taking parameters of $m_{eff} \approx 4 \times 10^{-14}$ kg and $\omega/(2\pi) = 7.01$ GHz. We use this method to obtain the value of the T_e when the membrane is artificially heated up by external white noise. In this work, the maximum vlues of the measured spectra density is ~ 1 nm$/\sqrt{Hz}$.

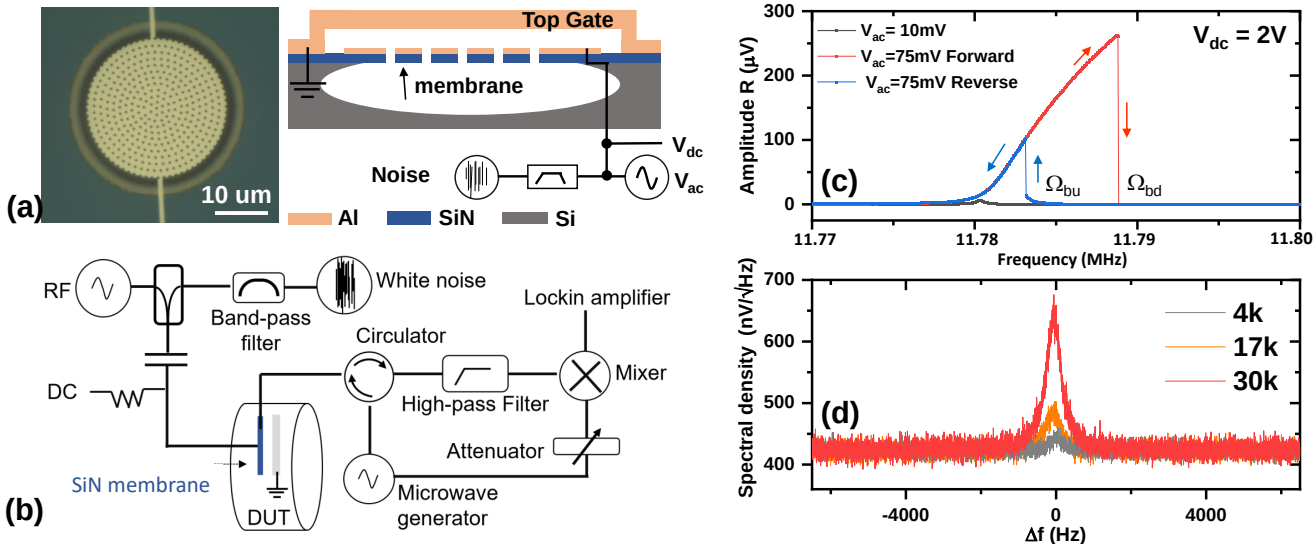

FIG. 1. (a) Left, an optical image of a silicon nitride membrane, covered with an Al thin film ∼25 nm in thickness. The silicon nitride (SiN) membrane is released from Si substrate by reactive ion etching un-wanted silicon nitride parts, circular holes (∼ 300 nm in diameter), followed with XeF_2 selective etching of the Si layer below the silicon nitride layer through those holes. Right, schematic diagram of the device in lateral view. Note that SiN is silicon nitride. (b) The measurement setup. A silicon nitride membrane is driven by means of an electrostatic force through combing *dc* and *ac* signals, and stochastic forces generated by a Gaussian white noise which is filtered to have a band-pass around resonance frequency of the desired mechanical mode. All measurements are performed at room temperature, in vacuum (pressure $< 10^{-6}$ mbar). (c) Black line, linear response of silicon nitride membrane, measured with $V_{dc} = 2$ V, $V_{ac} = 1$ mV$_p$ for the fundamental mode Ω_{01}. Both blue and red lines show the Duffing responses, which are measured with the higher driving amplitude, $V_{dc} = 2$ V, $V_{ac} = 75$ mV$_p$. The hysteresis regime is formed between forward (red line) and the backward (blue line) frequency sweeps. (d) Spectral density of the membrane's displacements, at different effective temperature T_e.

III. EXPERIMENTAL RESULTS AND DISCUSSION

In order to investigate the switching dynamics of the system in this room temperature measurement, we prepare a small hysteresis window of nonlinear responses to prepare bistable states. In this experiment, it is a challenge to observe the detected signal switching between low- and high- amplitudes in the large hysteresis window, e.g. a width much larger than 100 Hz. It could be due to the mechanical resonance frequency drifting at room temperature. Thus, the width is controlled to be less than 100 Hz by regulating amplitude of the f_d, as shown in Fig.2 (a). The typical value of the detected mechanical displacement in this nonlinear region is ∼ 38 nm. Without injecting extra white noise, stochastic switching between bistable states has been observed by setting the frequency of the driving force in the hysteresis regime. Amplitudes of the detected signals switch between two states, corresponding to the low ("L") and the high ("H") amplitude, as shown in Fig.2 (b)-(d). When the driving frequency is biasing at the center of the hysteresis window, the residence of each state exhibits almost equal probability, as shown in Fig. 2 (c). Whereas one of the states is more likely to be occupied when the frequency of the driving force is detuned from the center, even for only a few Hz, as presented in Fig. 2 (b) and (d). The probability of the occupation states exhibits high sensitivity to the driving frequency. This is because the double-well potential, in descriptions of bistable states, has been tilted by the frequency of the periodic driving force, f_d.

From the previous reports [29], we know that the switching rate Γ in the stochastic switching between the bistable states follows Kramer's law,

$$\Gamma = \Gamma_0 \, exp(\frac{-E_a}{k_B T_e}). \tag{3}$$

The Γ_0 is the maximum switching rate, E_a is an activation energy corresponding to the barrier height between bistable states [19]. For Duffing oscillators, the width of hysteresis window $|\Omega_{bd} - \Omega_{bu}|$ and the driving frequency Ω_d are supposed to play important role in manipulating the E_a and the Γ_0. In the switching process, the distribution of residence time (τ) corresponding to the "L" or "H" state follows a Poisson law,

$$N(\tau) = I \cdot \Gamma \, exp(-\tau\Gamma). \tag{4}$$

Here, the I is a parameter for normalizing the residence time distribution. The probability of residence in each state is therefore sensitive to the driving frequency.

Thus, we first measure the distributions of the residence time for both "L" and "H" occupation states corresponding to each value of the T_e. To do so, we exploit two forces to drive the membrane. The periodic driving force

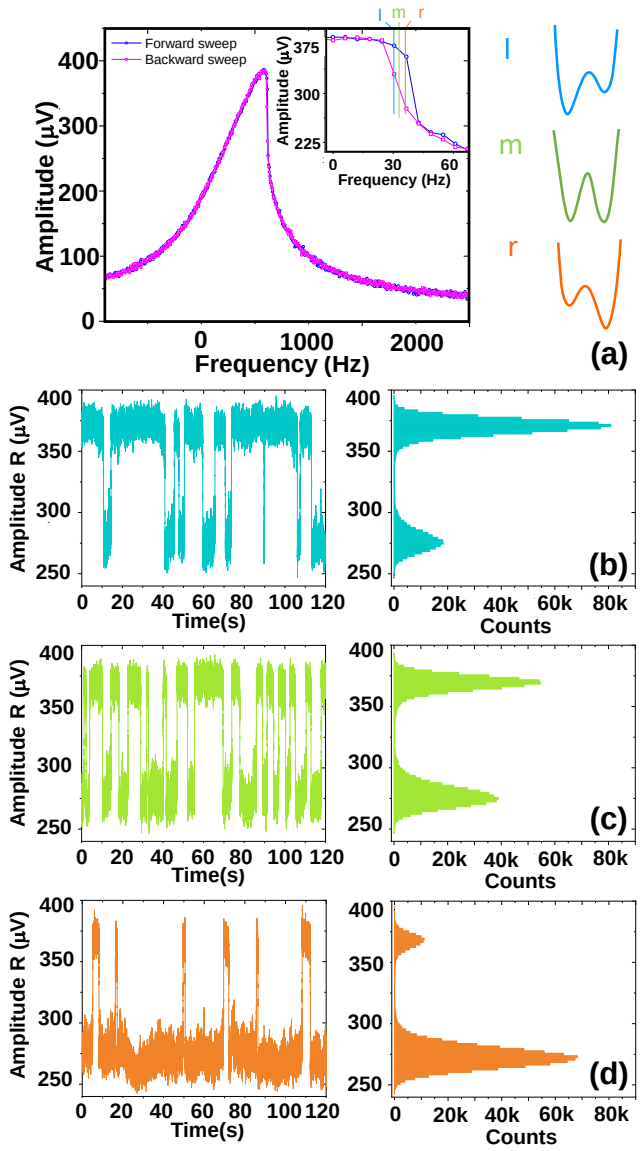

FIG. 2. (a) Left, without adding extra white noise, nonlinear responses of the forward and backward frequency sweeps, which are measured with a high driving force generated by $V_{dc} = 2$ V and $V_{ac} = 9$ mV_p, . Inset, zoom of the hysteresis frequency window, around 15 Hz in width. Right, schematic diagram of double wells corresponding to three different driving frequencies in bistable region, which is marked on the inset figure as "l", "m", and "r" respectively. (b)-(d) The left side of figures show amplitudes as a function of the measurement time in this stochastic system, driving respectively at "l", "m", and "r", as marked in the inset of the (a). Their histograms of the distributions in amplitudes are shown on the right side.

f_d with frequency Ω_d is used to control the width of hysteresis window and bistable states are prepared by driving membrane at the frequency $\Omega_d \sim (\Omega_{bd} - \Omega_{bu})/2$. The stochastic force f_n generated by white noise is employed to control the effective temperature T_e of the mechanical mode, by artificially "heating up" the membrane. By

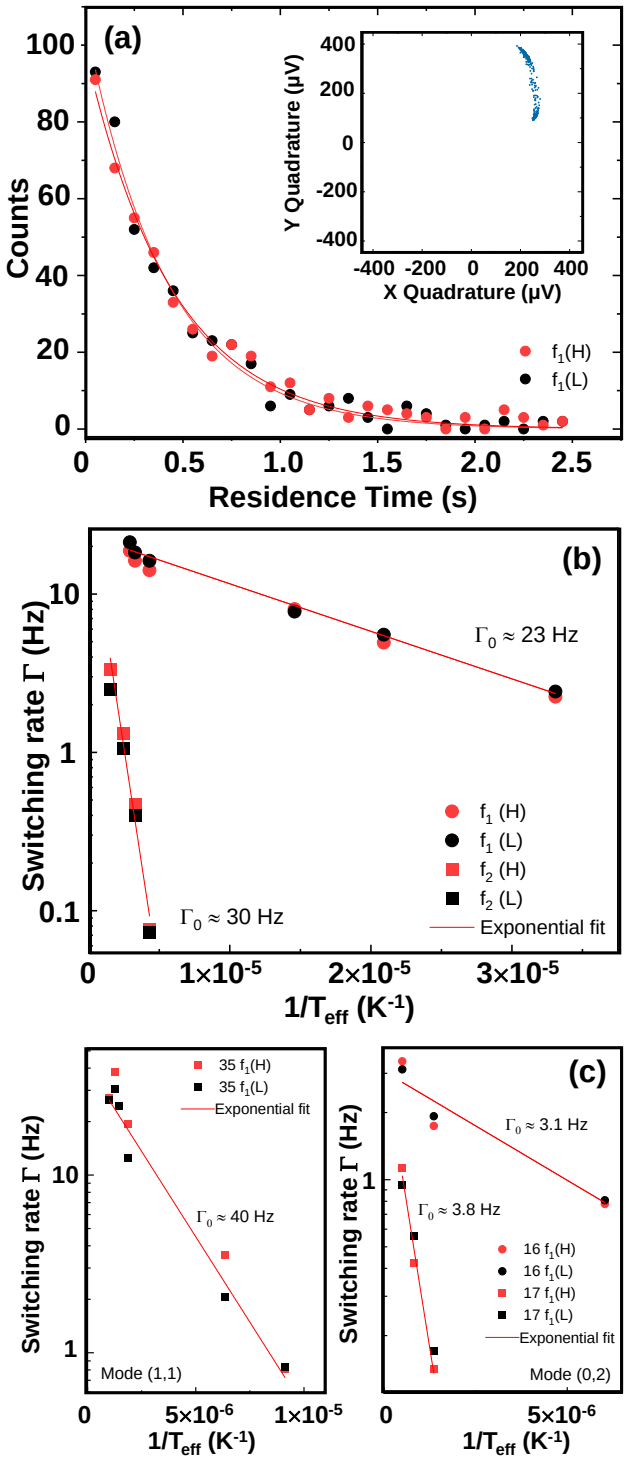

FIG. 3. (a) Residence time distributions for both "L" and "H" states at $T_e \approx 3 \times 10^4$ K. The red curves are fit by Poisson distribution function, giving a value of switching rate $\Gamma \approx 2.2$ Hz. The inset figure is amplitude distributions of detected signals shown in the two quadrature space and each point is one sample in the measurement of amplitude as a function of time. (b) Switching rate Γ of both states as a function of T_e^{-1}, corresponding to different driving forces. In both (a) and (b), the driving force f_1, f_2 are generated through combing $V_{dc} = 2$ V with $V_{ac} = 14$ mV_p, and 18 mV_p, respectively. (c) Left and Right show Γ versus $1/T_e$ for mechanical mode (1,1) and (0,2). These driving forces are normalized with f_1.

measuring the time trace of the detected signal amplitudes, we can make statistics of residence time. Figure 3 (a) shows distributions of residence time for both "L" and "H" states exhibit equal counts, which are measured at $T_e \approx 3 \times 10^4$ K. The inset figure shows amplitudes of the signal in a two-quadrature space, which presents bistable states of the membrane. These results indicates that potential well is controlled to be symmetric. Then, by using Poisson's law to fit the distribution of residence time, we can obtain the transition rate Γ corresponding to different T_e.

Figure 3 (b) shows exponential plots of Γ as functions of $1/T_e$ for the fundamental mode (0,1), corresponding to different widths of the hysteresis window controlled by the driving force f_d. The maximum switching rate Γ_0 can be obtained by exploiting Kramer's law as described by Eq.3. The value of $\Gamma_0 \approx 23$ Hz is obtained when the width of the hysteresis window $(\Omega_{bd} - \Omega_{bu})/2/\pi$ is controlled to be 18 Hz by the driving force f_1. The relatively higher value of $\Gamma_0 \approx 30$ Hz is obtained by using the higher force f_2, yielding the relatively wider hysteresis window with width $(\Omega_{bd} - \Omega_{bu})/2/\pi = 67$ Hz. Besides, we also measured the switching rate of the higher mechanical modes, (1,1) and (0,2), as shown in Fig. 3 (c). In the measurement of the mode (1,1), a similar width of hysteresis window, around 62 Hz, has been set and we obtain $\Gamma_0 \approx 40$ Hz. While, for the mode (0,2), the hysteresis window is controlled to be quite small, less than 10 Hz, and the measured values of Γ_0 are ≈ 3.1 Hz and 3.8 Hz, well below the damping rate of mechanical resonator, $\gamma_m/(2\pi)$. These measurement results indicate that the maximum value of switching rate between bistable states relies on the hysteresis window $(\Omega_{bd} - \Omega_{bu})$, in accordance with theoretical descriptions [18, 29]. Besides, we also found that the slope of these plots is sensitive to the amplitude of the driving force f_d, as shown in the Fig.3(b)-(c). From Kramer's law, we know that these slopes are proportional to the activation energy E_a. Therefore, these measurement results demonstrate that the activation energy E_a is also sensitive to the driving force, which is in accordance with Dykman's theoretical descriptions [29].

In theoretical analysis of stochastic switching in Duffing oscillators, it has been predicted that both of E_a and Γ_0 rely on several experimentally accessible parameters, such as driving force f_d, and frequency detuning between the driving frequency Ω_d and the bifurcation point Ω_{bd} [18, 29]. Therefore, we make a quantitative comparison between our experimental results and the theoretical expressions, the barrier height $E_a \propto f_d^2(\Omega_{bd} - \Omega_d)^{\frac{3}{2}}/(\Omega_{bd} - \Omega_m)^{\frac{5}{2}}/\gamma_m$ and the switching rate $\Gamma_0 = |\Omega_{bd} - \Omega_d|^{\frac{1}{2}}(\Omega_{bd} - \Omega_m)^{\frac{1}{2}}/(2\pi)$ [18]. From slopes of two curves shown in the Fig. 3 (b), we have obtained $E_a(f_2)/E_a(f_1) \approx 19.4$, in accordance with calculation results of 18.2. However, for the switching rate Γ_0, the calculation result of $\Gamma_0(f_1) \approx 148$ Hz and $\Gamma_0(f_2) \approx 71$ Hz are nearly ≈ 5 times and ≈ 2.3 times higher than our measurement results, respectively. Consequently, it

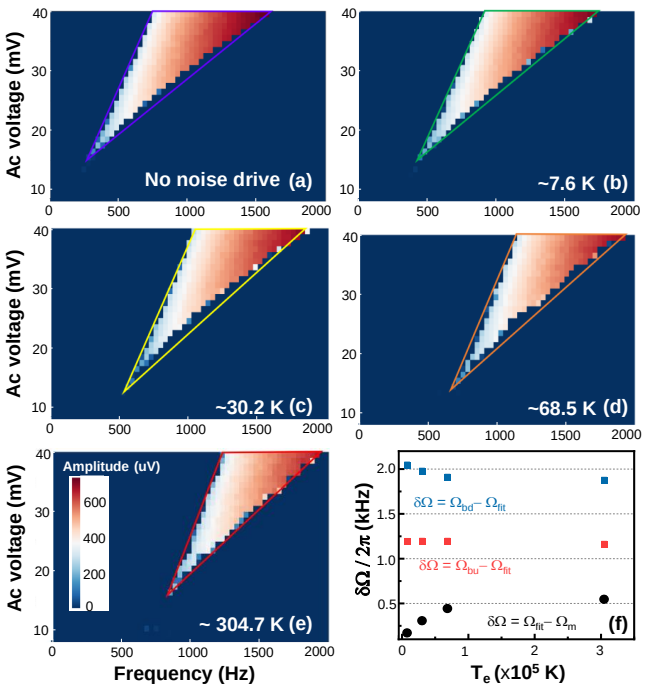

FIG. 4. The measurement of the nonlinear responses for the first mode is performed at a fixed *dc* voltage $V_{dc} = 2V$. (a)-(e) Hysteresis of 2D (two dimensional) plots corresponding to different noise drive power, in the form of the effective mode temperature. Each hysteresis curve is obtained from both forward and backward frequency sweeps at a fixed V_{ac} voltage. All 2D plots share the same color bar of the (e). Here, the sweeping frequency is normalized by the starting point. (f) $\delta\Omega$ as a function of mechanical mode temperature, where $\delta\Omega = \Omega_{bd} - \Omega_{fit}$ are plotted as blue squares for the forward and $= \Omega_{bu} - \Omega_{fit}$ are marked as red squares for backward sweeps respectively, measured at $V_{ac} = 40$ mV. The black dots correspond to $\delta\Omega = \Omega_{fit} - \Omega_m$. Here, we choose Ω_m as the reference frequency when there is no extra white noise.

gives $\Gamma_0(f_2)/\Gamma_0(f_1) \approx 2$, higher than the value of ≈ 1.3 obtained in measurement. Besides of Duffing nonlinear term in 1, other nonlinearities could cause this discrepancy, such as nonlinear damping or resorting forces [18]. Although it is difficult to have a quantitative agreement in comparisons, measurement results exhibit qualitative accordance with theoretical descriptions.

Besides of the noise assisted random jumps in bistable states, white noise induced stochastic force affecting on mechanical properties in nonlinear region are also deserved to be investigated. Therefore, we track the variations of hysteresis window in a fixed sweeping range for both the frequency and the V_{ac}, when increase the amplitude of stochastic force in the form of the effective temperature T_e. Figure 4 (a)-(e) show the 2D plots of hysterics regime, corresponding to different T_e. Each hysteric region is obtained by subtracting the data of the backward frequency sweep from the forward one. With increasing stochastic force, it is clear that the hysteresis window shifts towards to the higher frequency re-

gion. Here, we choose the hysteresis region, which consisting of forward and backward frequency sweeps and are measured at the $V_{ac} = 40$ mV, for further analysis. By fitting each nonlinear curve, the resonance frequency Ω_{fit} is obtained and we find that it shifts towards the higher frequencies as T_e increases. Moreover, variations of bifurcation points as a function of T_e have also been observed through definitions of $\delta\Omega = \Omega_{bd} - \Omega_{fit}$ and $\delta\Omega = \Omega_{bu} - \Omega_{fit}$. These analyses are shown in Fig. 4(f).

Compared with Ω_{bu}, the Ω_{bd} seems to be more sensitive to stochastic forces. For a Duffing oscillator, driven by a periodic force $f_d(t)$, it is well-known that the bifurcation point Ω_{bd} (for the case of spring hardening effect) can be generally described by $\Omega_{bd} = \Omega_m(1 + \frac{3\alpha}{8k}x_{max}^2)$ [30]. It depends on the Duffing parameter α, the maximum mechanical displacement x_{max}, and the spring constant $k = \Omega_m^2 m_{eff}$. From Fig. 4 (b)-(e), we did not observe clearly variations in amplitudes at Ω_{bd}. Besides, for circular membrane, Duffing (hardening) nonlinear coefficient α, is mainly dominated by geometry [31]. Therefore, the displacements of the hysteresis window can be attributed to the modulations of spring constant by stochastic forces. Besides observations of hysteresis windows shifting, we also find that the width of hysteresis window starts to be reduced as the amplitude of stochastic force increases. Similar phenomenon has been reported in previous studies of doubly-clamped beams with [19] and micro-cantilever [12] increasing amplitude of stochastic force, which also has been attributed to stochastic forces affecting the spring constant of the mechanical resonator. However, compared with these previous reports, we did not observe the hysteresis quenched even though the membrane is artificially heated at same orders of the T_e. We suppose that it requires the much higher value of the f_n to quench hysteresis regime. Because this high stressed silicon nitride membrane, with a fully clamped scheme, has the higher spring constant $k \sim 90$ N/m [22].

IV. CONCLUSION

In conclusion, we have investigated the effect of stochastic forces on the Duffing nonlinear behaviors of silicon nitride membrane nanoelectromechanical resonators, by using microwave interferometry detection scheme at room temperature. In the hysteresis region, the probability of occupying a state exhibits high sensitivity to the driving frequency, demonstrating the potential to explore nonlinear-based sensing. The stochastic switching of the membrane, corresponding to different mechanical modes, has been found to follow Kramer's law. Our measurements are in qualitative agreement with the theoretical descriptions of the maximum switching rate Γ_0 and activation energy E_a influenced by the experimental setting of the driving force and the width of the hysteresis window. Besides, squeeze of Duffing hysteresis window and shifts of bifurcation points have also been observed when increasing the effective temperature T_e and been attributed to stochastic forces influencing the spring constant of the membrane. Although the typical values of the Γ_0 obtained in this experiment is in the orders of tens Hz, these studies pave way for explorations of stochastic switching based novel functions beyond sensing, such as random number generators, stochastic computing, and logic gates [3–5, 17].

ACKNOWLEDGMENTS

We would like to acknowledge financial support from STaRS-MOC Project No. 181386 the Region Hauts-de-France, from ISITE-MOST Project No. 201050, and the French National Research Agency, ANR-MORETOME, No. ANR-22-CE24-0020-01. This work was partly supported by the French Renatech network.

[1] L. Gammaitoni, P. Hänggi, P. Jung, and F. Marchesoni, Stochastic resonance, Reviews of modern physics **70**, 223 (1998).
[2] R. L. Badzey and P. Mohanty, Coherent signal amplification in bistable nanomechanical oscillators by stochastic resonance, Nature **437**, 995 (2005).
[3] D. Vodenicarevic, N. Locatelli, A. Mizrahi, J. S. Friedman, A. F. Vincent, M. Romera, A. Fukushima, K. Yakushiji, H. Kubota, S. Yuasa, *et al.*, Low-energy truly random number generation with superparamagnetic tunnel junctions for unconventional computing, Physical Review Applied **8**, 054045 (2017).
[4] S. Gaba, P. Sheridan, J. Zhou, S. Choi, and W. Lu, Stochastic memristive devices for computing and neuromorphic applications, Nanoscale **5**, 5872 (2013).
[5] F. Zahari, E. Pérez, M. K. Mahadevaiah, H. Kohlstedt, C. Wenger, and M. Ziegler, Analogue pattern recognition with stochastic switching binary cmos-integrated memristive devices, Scientific reports **10**, 1 (2020).
[6] K. Wiesenfeld and F. Moss, Stochastic resonance and the benefits of noise: from ice ages to crayfish and squids, Nature **373**, 33 (1995).
[7] P. R. Muppalla, O. Gargiulo, S. Mirzaei, B. P. Venkatesh, M. Juan, L. Grünhaupt, I. Pop, and G. Kirchmair, Bistability in a mesoscopic josephson junction array resonator, Physical Review B **97**, 024518 (2018).
[8] D. Wales *et al.*, *Energy landscapes: Applications to clusters, biomolecules and glasses* (Cambridge University Press, 2003).
[9] M. Spano, M. Wun-Fogle, and W. Ditto, Experimental observation of stochastic resonance in a magnetoelastic ribbon, Physical Review A **46**, 5253 (1992).
[10] W. Wernsdorfer, K. Hasselbach, A. Benoit, B. Barbara, B. Doudin, J. Meier, J.-P. Ansermet, and D. Mailly, Mea-

surements of magnetization switching in individual nickel nanowires, Physical Review B **55**, 11552 (1997).
[11] C. Stambaugh and H. B. Chan, Noise-activated switching in a driven nonlinear micromechanical oscillator, Physical Review B **73**, 172302 (2006).
[12] W. J. Venstra, H. J. Westra, and H. S. Van Der Zant, Stochastic switching of cantilever motion, Nature communications **4**, 1 (2013).
[13] O. Maillet, X. Zhou, R. Gazizulin, A. M. Cid, M. Defoort, O. Bourgeois, and E. Collin, Nonlinear frequency transduction of nanomechanical brownian motion, Physical Review B **96**, 165434 (2017).
[14] X. Zhou, D. Cattiaux, R. Gazizulin, A. Luck, O. Maillet, T. Crozes, J.-F. Motte, O. Bourgeois, A. Fefferman, and E. Collin, On-chip thermometry for microwave optomechanics implemented in a nuclear demagnetization cryostat, Physical Review Applied **12**, 044066 (2019).
[15] G. Dion, S. Mejaouri, and J. Sylvestre, Reservoir computing with a single delay-coupled non-linear mechanical oscillator, Journal of Applied Physics **124**, 152132 (2018).
[16] R. Gazizulin, O. Maillet, X. Zhou, A. M. Cid, O. Bourgeois, and E. Collin, Surface-induced near-field scaling in the knudsen layer of a rarefied gas, Physical Review Letters **120**, 036802 (2018).
[17] D. N. Guerra, A. R. Bulsara, W. L. Ditto, S. Sinha, K. Murali, and P. Mohanty, A noise-assisted reprogrammable nanomechanical logic gate, Nano letters **10**, 1168 (2010).
[18] M. Defoort, V. Puller, O. Bourgeois, F. Pistolesi, and E. Collin, Scaling laws for the bifurcation escape rate in a nanomechanical resonator, Physical Review E **92**, 050903 (2015).
[19] J. Aldridge and A. Cleland, Noise-enabled precision measurements of a duffing nanomechanical resonator, Physical review letters **94**, 156403 (2005).
[20] R. J. Dolleman, P. Belardinelli, S. Houri, H. S. van der Zant, F. Alijani, and P. G. Steeneken, High-frequency stochastic switching of graphene resonators near room temperature, Nano letters **19**, 1282 (2019).
[21] A. Chowdhury, S. Barbay, M. G. Clerc, I. Robert-Philip, and R. Braive, Phase stochastic resonance in a forced nanoelectromechanical membrane, Physical Review Letters **119**, 234101 (2017).
[22] X. Zhou, S. Venkatachalam, R. Zhou, H. Xu, A. Pokharel, A. Fefferman, M. Zaknoune, and E. Collin, High-q silicon nitride drum resonators strongly coupled to gates, Nano Letters **21**, 5738 (2021).
[23] A. Pokharel, H. Xu, S. Venkatachalam, E. Collin, and X. Zhou, Capacitively coupled distinct mechanical resonators for room temperature phonon-cavity electromechanics, Nano Letters **22**, 7351–7357 (2022).
[24] M. Yuan, M. A. Cohen, and G. A. Steele, Silicon nitride membrane resonators at millikelvin temperatures with quality factors exceeding 108, Applied Physics Letters **107**, 263501 (2015).
[25] T. R. Albrecht, P. Grütter, D. Horne, and D. Rugar, Frequency modulation detection using high-q cantilevers for enhanced force microscope sensitivity, Journal of applied physics **69**, 668 (1991).
[26] A. A. Clerk, M. H. Devoret, S. M. Girvin, F. Marquardt, and R. J. Schoelkopf, Introduction to quantum noise, measurement, and amplification, Reviews of Modern Physics **82**, 1155 (2010).
[27] B. Hauer, C. Doolin, K. Beach, and J. Davis, A general procedure for thermomechanical calibration of nano/micro-mechanical resonators, Annals of Physics **339**, 181 (2013).
[28] X. Zhou, D. Cattiaux, D. Theron, and E. Collin, Electric circuit model of microwave optomechanics, Journal of Applied Physics **129**, 114502 (2021).
[29] M. Dykman and M. Krivoglaz, Theory of fluctuational transitions between stable states of a nonlinear oscillator, Sov. Phys. JETP **50**, 30 (1979).
[30] R. Lifshitz and M. C. Cross, Nonlinear dynamics of nanomechanical and micromechanical resonators, Reviews of nonlinear dynamics and complexity **1** (2008).
[31] D. Cattiaux, S. Kumar, X. Zhou, A. Fefferman, and E. Collin, Geometrical nonlinearity of circular plates and membranes: An alternative method, Journal of Applied Physics **128**, 104501 (2020).
[32] M. Dykman, *Fluctuating nonlinear oscillators: from nanomechanics to quantum superconducting circuits* (Oxford University Press, 2012).